The phase equilibria in the Au-In-Ga ternary system

Ghasemi, Masoomeh; Lidin, Sven; Johansson, Jonas

Published in:
Journal of Alloys and Compounds

DOI:
10.1016/j.jallcom.2013.11.088

2014

The phase equilibria in the Au-In-Ga ternary system

Masoomeh Ghasemi[1], Sven Lidin[2], Jonas Johansson[1]

1 Solid State Physics, Lund University, Box 118 SE-22100 Lund, Sweden

2 Polymer and Materials Chemistry, Lund University, Box 124, SE-22100 Lund, Sweden

Corresponding author:

Email: masoomeh.ghasemi@ftf.lth.se
Phone: 0046-462220586
Address: Box 118, SE-22100 Lund, Sweden

Email addresses:

masoomeh.ghasemi@ftf.lth.se
sven.lidin@chem.lu.se
jonas.johansson@ftf.lth.se

Abstract

The phase equilibria of the Au-In-Ga system were investigated for the first time using Differential Thermal Analysis (DTA), X-Ray Diffractometry (XRD), Energy Dispersive X-ray Spectroscopy (EDS) and Scanning Electron Microscopy (SEM). A new ternary phase (Au_2InGa_2) with the hexagonal structure ($P6_3/mmc$) was discovered which melts incongruently at 394 °C. From the experimental results, several invariant reactions have been identified and discussed.

Keywords: phase diagrams; thermodynamic properties; thermodynamic modeling, semiconductors.

1. Introduction

Due to the potential and promising application of one-dimensional (1D) semiconductor nanostructures, so-called nanowires (NWs), in electronic and optoelectronic devices [1, 2], the thermodynamics of the constituting materials systems are of interest. In the most common growth mechanism, Vapor-Liquid-Solid (VLS) growth, 20-100 nm Au particles (in liquid phase) on a crystalline substrate act as catalyst, on one hand, to stimulate the decomposition of precursors (in gas phase) on the particle surface and as solvent, on the other hand, to dissolve the precursors and to drive the subsequent growth of NWs (in solid phase) at the interface between the Au particle and the substrate [3, 4]. One of the material systems of interest is the III-V heterostructure NWs containing Ga and In, e.g. axial sequential growth of InAs on GaAs [5-7]. Since a thermodynamic description of the ternary Au-In-Ga system is lacking in the literature, we aimed at investigating the phase equilibria in order to provide a thermodynamic assessment of this system and to understand the optimal growth condition of NWs. The influence of group V has been ignored and the reason for this is that the solubilities of the common group V elements (As and P) in Au are negligible.

To the best of our knowledge, this article reports for the first time a thorough investigation of the ternary phase equilibria of the Au-In-Ga system. The only report on ternary Au-In-Ga alloys that we have found in the literature was presented in 1978 by Hoyt and Mota [8]. They studied the dependence of T_c (Curie temperature) on the elastic energy of Au-In-Ga alloys. The lattice parameter of the alloys with fixed gold composition of 92 at.% with varying amount of In and Ga (0-8 at%) was measured to study the correlation between the lattice parameters and T_c. The only investigated solid phase in their report was the fcc phase for which the lattice parameters of the alloys were reported. Thus, no previous comprehensive experimental investigation or modeling of the Au-In-Ga ternary system in the scope of phase diagram assessment has been reported.

The aim of the present study was to investigate the phase equilibria of the Au-In-Ga ternary system using complementary techniques including Differential Thermal Analysis (DTA), X-Ray Diffractometry (XRD), Energy Dispersive X-ray Spectroscopy (EDS) and Scanning Electron Microscopy (SEM). The experimental results will be used for further thermodynamic assessment of this ternary system.

As a starting point, we calculated the Au-In-Ga ternary phase diagram from the constituent binaries without any ternary terms. Based on such a calculated isothermal section of the phase diagram at 280 °C, a number of samples varying in composition were chosen for measurements. The most significant result was the identification of the new ternary phase, Au_2InGa_2, with a hexagonal structure which melts incongruently at 394 °C. Moreover, a number of key reactions were also identified and discussed. The results guided us for the further assessment of the thermodynamic description of the system which will be published elsewhere. Moreover, the results will also be of importance for understanding the processes in the gold alloy particle during NW growth.

2. Experimental

Pure metal foils of Au and In (both 99.999 mass%) and pure lumps of Ga (99.9999 mass%) were used to prepare alloys of the required compositions. Samples with a total mass of about 0.2-0.3g were weighed and mixed in alumina crucibles. The crucibles were transferred into quartz tubes and these were evacuated (~10^{-5} mbar). The reason to keep the samples in alumina crucibles was to prevent the reaction of Ga with silica at high temperatures [9]. The samples were heated to 1100°C, slightly higher than the melting point of Au, kept at that temperature for one night and subsequently annealed at 280°C (except for samples 1-4 which were annealed at 300°C) for one to three weeks (see table 1). Finally the samples were slowly

cooled down to room temperature. All samples were analyzed using DTA, XRD and SEM/EDS.

For DTA measurements (Jupiter F3 449, Netzsch Co.), a piece of sample with the mass of about 50 to 100 mg in an alumina crucible under N_2 flow was used. The reference was an empty alumina crucible. The furnace was evacuated and flushed with N_2 three times before thermal cycles to prevent the oxidation. The heating and cooling rate was 10 °C/min. As an extra precaution a few samples were also measured at the rate of 5 °C/min where no extra thermal effect was observed.

For powder XRD measurements (STOE Stadi P, Cu-kα radiation) a piece of alloy was ground. The powder was transferred to a quartz tube and was then annealed in the sealed tube at 280°C for about three days. The XRD machine was first calibrated using Si powder. Then, the sample powders were measured with steps of 0.9 of the detector and 100 s exposure time.

The crystal structure of several samples (4, 23, 25, 26) was analyzed using single crystal X-ray diffraction measurements. For these measurements a small piece of sample was mounted on a glass fiber with epoxy glue. The single crystal measurement was then performed at ambient condition on an Agilent Technologies Xcalibur E instrument.

To investigate the microstructure of the samples, both optical (Nikon Optiphot) and scanning electron microscopes (JSM-6700F SEM) were employed. The electron microscope was also equipped with an Oxford EDS system which was used to measure the local chemical compositions of coexisting phases. For these characterizations, samples were embedded into a conductive resin and were then polished in three steps with diamond suspensions (9 μm and 1 μm) and finally with a SiO_2 colloidal suspension.

3. Results and Discussion

The ternary phase diagram of the Au-In-Ga system was constructed from constitutent binaries using the CALPHAD method [10] with Thermo-Calc software [11] without including any ternary parameter. The Au-Ga binary description was taken from Wang *et al.* [12]. The Au-In binary phase diagram studied by Liu *at al*. [13] was used. In the case of the simple In-Ga binary system, the description by Andersson and Ansara [14] was used.

An isothermal section of the calculated ternary phase diagram of the Au-In-Ga system at 280 °C (the same as the annealing temperature) and the sub-binaries are shown in Figure 1. In total, 26 samples with varying compositions (marked on the ternary phase diagram in Figure 1) were chosen in an attempt to investigate all regions of interest in the phase diagram. After melting and homogenizing the samples, they were measured with the techniques described in the previous section. The details of the experimental conditions and the results are summarized in Table 1.

Regarding the DTA measurement, to make sure of reproducibility of the results, the heating and cooling cycles were repeated three times for each sample. Due to large undercooling effects only temperatures on heating curves were considered for further optimization of the thermodynamic modeling. In general, the first heating cycle was ignored and the mean value of temperatures on the second and third curves was taken as the phase transition or the liquidus temperatures. The experimental error of the measured temperatures on consecutive DTA curves was in the order of ±0.5°C. The result was analyzed using the thermal analysis software which has been delivered with the DTA equipment (NETZSCH Proteus- Thermal Analysis- version 5.1.0). On heating curves, the onset temperature was used for the first thermal event. For next thermal events, the peak maximums were registered. For the registered temperatures on cooling curves in Table 1, the onset was used.

Using the powder diffraction data, the coexistence of phases, the qualitative phase fractions and the lattice parameters were detected using the JANA2006 software [15]. Moreover, due to the shift in diffraction peaks of known phases to higher or lower angles, it was found that there is some solubility of the third element in some binary phases. This was also verified by EDS results; according to that, the average value of solubility of Ga in $AuIn_2$ and In in $AuGa_2$ was about 9.5 at.% and 5.5 at.% , respectively whereas that of all other binary phases was less than 4.0 at.% (see Table 1).

The most important result of the powder and single crystal XRD measurements and microstructural observations was the discovery of a new ternary phase which occurs at a gold content of about 40.0 at.%. Using the powder XRD data, it was found that the ternary phase, Au_2InGa_2, has a hexagonal structure which belongs to $P6_3/mmc$ space group with the lattice parameters of $a = 4.20473(16)$ Å and $c = 12.9673(5)$ Å. It melts incongruently at about 394 °C. The details of characterization and the structure refinement of this new ternary compound as well as its electronic structure and chemical bonding is published elsewhere [16].

According to the DTA results, several invariant reactions were identified. Table 2 summarizes a list of invariant reactions that are discussed in this report.

Figure 2 shows the SEM micrograph and the DTA thermogram of sample 16. The presence of four solid phases: $AuIn_2$, Au_2InGa_2, AuIn and AuGa in the SEM micrograph indicates the non-equilibrium state of the sample due to a peritectic reaction. Three thermal events are recorded in the thermogram which are more clearly separated on the cooling curve. On cooling, first, $AuIn_2$ and liquid react to form Au_2InGa_2 at 393 °C (corresponding to 391 °C on the heating curve). According to thermodynamic modeling, two invariant reactions are suggested to occur after that. At 363 °C, AuIn begins to from peritectically through the

reaction L + $AuIn_2$ + Au_2InGa_2 ↔ AuIn (P11). This reaction is registered at 386 °C on the heating curve. Next, the invariant reaction L ↔ Au_2InGa_2 + AuIn + AuGa (E3) occurs at 355 °C on cooling and correspondingly at 375 °C on heating.

Similar thermal events were also observed in samples 10, 14, 16, 17 and 25. However, due to the sluggish nature of these reactions there were discrepancies between the registered temperatures on the DTA curves of different samples. Thus, in case of the reaction P9, the average value of the registered temperatures on heating curves of sample 14 and 25 where the peak temperatures are clearly distinguishable (Figure S1 in supplementary information) is reported as the reaction temperature, 394.0 °C. The other two events, P11 and E3 occur at close temperatures, hence that might be the reason that they are not registered in DTA curves of all mentioned samples. However, all three reactions, P9, P11 and E3 are registered in both heating and cooling DTA curves of samples 16 (Figure 2) and 17 (not shown here). Therefore, the average value of the maximum peak temperatures on the heating curves of these samples is reported as the reaction temperatures in Table 2.

The quasi-binary eutectic reaction L ↔ $AuIn_2$ + $AuGa_2$ was registered at 432 °C in the thermogram of sample 13. The SEM image and the DTA micrograph are shown in Figure 3.a and b, respectively. The heating curve shows only one pronounced peak. The small shoulder after the peak temperature on the heating curve is probably the liquidus temperature of $AuIn_2$ which is close to the eutectic temperature at this composition. The same thermal event has also been recorded in the DTA curves of samples 10 and 14.

Another quasi-binary eutectic reaction at higher gold content of about 50.0 at.% is L ↔ AuIn + AuGa which was registered in thermograms of sample 8 at equal atomic composition of In and Ga. In Figure 3.d, the pronounced thermal effect on the heating curve at about 383 °C corresponds to the eutectic temperature. The SEM micrograph (Figure 3.c) shows the AuIn-

AuGa two-phase field. A small quantity of a third phase was also detected in the SEM micrograph which was Au_3In_2 based on the EDS spectra and the XRD data. Thus, the thermal event at 325 °C is possibly related to the crystallization of Au_3In_2 through the quasi-peritectic reaction P8: L + AuIn ↔ Au_3In_2 + AuGa which was also observed in DTA thermograms of samples 1, 2, 3 and 6. The reported temperature for this reaction in Table 2 is the average of the registered temperatures on DTA thermograms displaying this thermal event.

Figure 4 shows the SEM image of samples 23 and 24 at Ga content of 9.0 at.% as well as the corresponding DTA thermograms. For the more gold-rich sample 23, the crystals of the Au_7In_3 phase first begin to crystallize from the liquid phase on cooling. Next, the invariant reaction of formation of the AuGa phase (E1) occurs. These thermal events are registered at 419 °C and 305 °C on the heating curve, respectively. For the composition of sample 23, according to the thermodynamic modeling, the Au_3In_2 phase should be the first crystalline phase that forms after Au_7In_3. There is, however, a small thermal lag at 398 °C which might be related to the formation of Au_3In_2. This is clearer in the SEM image of sample 24 where the primary phase is Au_3In_2. The highest peak temperature at 398 °C on the heating curve of sample 24 should be the temperature at which Au_7In_3 and Au_3In_2 form the liquid phase. The thermal event at 305 °C is related to the formation of AuGa through the eutectic reaction L ↔ Au_7In_3 + AuGa + Au_3In_2 (E1). The same thermal event as the invariant reaction E1 was also observed in the thermogram of sample 5.

To make sure of consistency of results after thermal cycles, the post-DTA microstructures, compositions and diffraction patterns of several samples were recorded. In the case of XRD measurements, there was no discrepancy in the diffraction patterns of the samples before and after thermal cycles. As an example, the pre- and post-XRD patterns of sample 25 are shown in Figure S2 in the supplementary information. The microstructural and compositional

analysis of the post-DTA samples, on the other hand, showed the same coexisting phases but different grain sizes and microstructural patterns compared to pre-DTA samples. For instance, the pre- and post-DTA SEM micrographs of sample 3 shown in Figure 5, AuGa, Au_3In_2 and Au_7In_3 phases are coexisting, but the microstructural patterns differ in grain size and pattern.

4. Conclusion

The phase equilibria of the Au-In-Ga ternary system have been investigated for the first time (to the best of our knowledge). Based on pure extrapolation from sub-binaries an isothermal section of the ternary phase diagram at 280 °C was mapped using DTA, SEM/EDS and XRD methods. The results revealed the need for optimizing the thermodynamic description of this ternary system due to several reasons.

The first reason is the identification of a previously unknown ternary phase, Au_2InGa_2, which should be included into the thermodynamic description of the system. The new phase has a hexagonal closed packed crystal structure belonging to the space group $P6_3/mmc$ which forms peritectically at 394 °C. The structural properties of the new phase, which is a truly ordered phase, needed further consideration. Thus, the detail of the crystal structure along with an analysis of the electronic structure using first-principle calculations is reported elsewhere.

Second, the solubility of the third element in binary phases is not taken into account in the extrapolated database, whereas the experiments showed some level of solubility. Third, the liquidus temperatures and the temperatures of invariant reactions are not very-well predicted using the extrapolated database. Thus, the thermodynamic description of the Au-In-Ga system needs to be optimized and the details of this will be outlined elsewhere.

These new results increase the understanding of the state of the gold alloy particle during growth of Ga and In based III-V semiconductor NWs, which is crucial for controlling their growth.

Acknowledgement

We gratefully acknowledge financial support from the Nanometer Structure Consortium at Lund University (nmC@LU), the Swedish Research Council (VR), and the Knut and Alice Wallenberg Foundation (KAW). We also thank Sören Jeppesen for excellent technical support.

References

[[1] R. Yan, D. Gargas, P. Yang, Nanowire photonics, Nat Photonics, 3 (2009) 569-576.

[2] L.E. Wernersson, C. Thelander, E. Lind, L. Samuelson, III-V Nanowires-Extending a Narrowing Road, P IEEE, 98 (2010) 2047-2060.

[3] J. Johansson, K.A. Dick, Recent advances in semiconductor nanowire heterostructures, CrystEngComm, 13 (2011) 7175-7184.

[4] R.S. Wagner, W.C. Ellis, VAPOR-LIQUID-SOLID MECHANISM OF SINGLE CRYSTAL GROWTH, Appl. Phys. Lett., 4 (1964) 89-90.

[5] M. Paladugu, J. Zou, J.N. Guo, X. Zhang, Y. Kim, H.J. Joyce, Q. Gao, H.H. Tan, C. Jagadish, Nature of heterointerfaces in GaAs/InAs and InAs/GaAs axial nanowire heterostructures, Appl. Phys. Lett., 93 (2008) 101911-101914.

[6] M.E. Messing, J. Wong-Leung, Z. Zanolli, H.J. Joyce, H.H. Tan, Q. Gao, L.R. Wallenberg, J. Johansson, C. Jagadish, Growth of Straight InAs-on-GaAs Nanowire Heterostructures, Nano Lett., 11 (2011) 3899-3905.

[7] K.A. Dick, J. Bolinsson, B.M. Borg, J. Johansson, Controlling the Abruptness of Axial Heterojunctions in III–V Nanowires: Beyond the Reservoir Effect, Nano Lett., 12 (2012) 3200-3206.

[8] R.F. Hoyt, A.C. Mota, Elastic strain energy dependence of Tc in ternary goldbased solid solutions, J. Less Common Metals, 62 (1978) 183-188.

[9] C.N. Cochran, L.M. Foster, Reactions of Gallium with Quartz and with Water Vapor, with Implications in the Synthesis of Gallium Arsenide, J. Electrochem. Soc., 109 (1962) 149-154.

[10] L. Lukas, S.G. Fries, B. Sundman, Computational Thermodynamics, The Calphad Method, Cambridge University Press, 2007.

[11] J.O. Andersson, T. Helander, L. Höglund, S. Pingfang, B. Sundman, Thermo-Calc & DICTRA, computational tools for materials science, Calphad, 26 (2002) 273-312.

[12] J. Wang, H.S. Liu, H.Y. Zhou, Z.P. Jin, Thermodynamic assessment of the Au–Ga binary system, Calphad, 35 (2011) 242-248.

[13] H.S. Liu, Y. Cui, K. Ishida, Z.P. Jin, Thermodynamic reassessment of the Au-In binary system, Calphad, 27 (2003) 27-37.

[14] T.J. Anderson, I. Ansara, The Ga-In (Gallium-Indium) System, J. Phase Equilib., 12 (1991) 64-72.

[15] V. Petricek, M. Dusek, L. Palatinus, Jana2006. The crystallographic computing system, in, Institute of Physics, Praha, Czech Republic, , 2006.

[16] M. Ghasemi, S. Lidin, J. Johansson, F. Wang, Bonding in intermetal l ics may be deceptive – The case of the new type structure Au_2InGa_2, Intermetallics, Accepted, (2013).

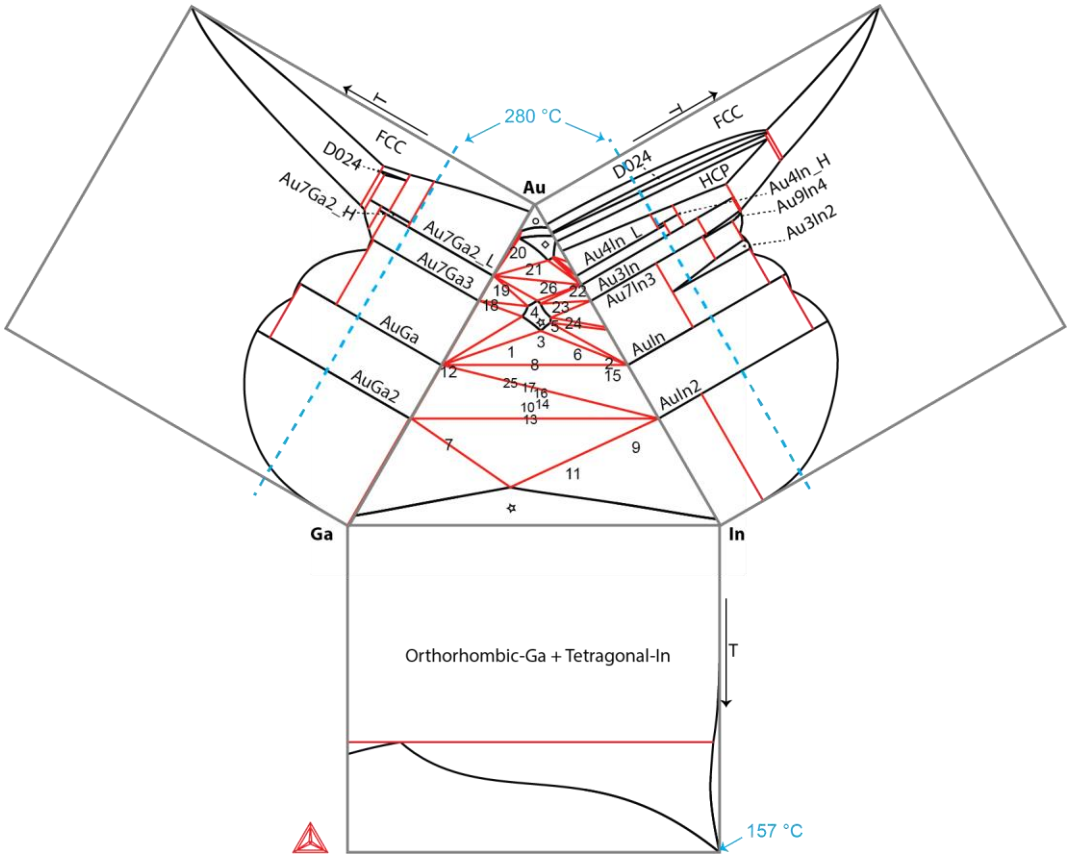

Figure 1. A calculated isothermal section of the Au-In-Ga ternary phase diagram at 280°C along with the constituting binary phase diagrams. The dashed lines correspond to 280 °C on the Au-In and Au-Ga binaries. The numbers on the ternary phase diagram correspond to the numbering of samples in Table 1. The signs indicate the single-phase domains; ☆, ◇ and ○ corresponding to liquid, $D0_{24}$ and fcc, respectively.

Table 1. The preparation details of samples and the experimental results of DTA, XRD and EDS measurements.

Sample	Nominal composition (at.%)			Heat treatment	Phases	EDS analysis (at.%)			Thermal effects (°C)	
	Au	In	Ga			Au	In	Ga	Heating	Cooling
1	53.7	19	29.3	300 °C, 5 days	Primary crystals of					
					AuGa	55.8	4.7	39.5	328	324
				DTA 5 and 10 °C/min	Small quantities of				363	345
					AuIn	53.1	42.0	4.9	390	368
					Au_3In_2	63.9	31.7	4.4		
2	50	45.1	4.9	300 °C, 5 days	Almost single phase					
					AuIn	52.2	43.8	4.0	326	311
				DTA 5 and 10 °C/min	Very small quantities of				485	417
					AuGa	54.2	4.2	41.6		
					Au_3In_2	63.5	33.0	3.5		
3	57.3	22.8	19.9	300 °C, 5 days	Primary phase of Au_3In_2	64.3	31.6	4.1	328	314
					AuGa	54.5	3.3	42.2		323
				DTA 5 and 10 °C/min	Au_7In_3	70.6	25.8	3.6		
4	66.2	16.7	17.1	300 °C, 5 days	Primary crystals of Au_7In_3	70.0	24.6	5.4	298	284
					Nucleation of AuGa	43.7	0.9	55.4	360	344
				DTA 5 and 10 °C/min	un-indexed (this sample locates as liquid phase based on modeling)	73.9	16.5	9.6		
5	62.2	24.6	13.2	280 °C, 5 days	Primary crystals of Au_3In_2	63.6	31.6	4.8	308	283
					Nucleation of AuGa and	54.0	2.0	44.0	378	368
				DTA 10 °C/min	Au_7In_3	69.8	26.0	4.2		
6	53.1	35.1	11.8	280 °C, 5 days	Primary phase of AuIn	52.8	42.2	5.0	330	305
					Nucleation of AuGa and	54.2	2.6	43.2	449	371
				DTA 10 °C/min	Au_3In_2	64.1	32.9	3		
7	25.2	14.5	60.3	280 °C, 5 days	Almost single phase $AuGa_2$				280	422
					* susceptible to oxidation				424	
				DTA 10 °C/min						
8	49.9	25	25.1	280 °C, 5 days	Two phase sample AuGa and	54.0	4.0	42.0	325	326
					AuIn	53.1	41.8	5.1	383	359
				DTA 10 °C/min	Very small quantity of	63.9	33.4	2.7		
					Au_3In_2					
9	24.3	65.2	10.5	280 °C, 5 days	Almost single phase $AuIn_2$				469	467
					Small quantity of In					
				DTA 10 °C/min						
10	37.1	30.9	32	280 °C, 5 days, sample not in equilibrium	Primary phase of Au_2InGa_2	45.5	19.6	34.9	390	371
					Nucleation of $AuIn_2$ and	36.1	52.6	11.3	435	414
				DTA 10 °C/min	$AuGa_2$	41	6.4	52.6		
11	16.1	52.2	31.7	280 °C, 5 days	Primary phase of $AuIn_2$					
					Some quantity of In					
				DTA 10 °C/min						
12	47.9	3.1	49	280 °C, 5 days	Primary crystals of AuGa	54.5	2.4	43.1	385	402
					and $AuGa_2$	40.7	6.4	52.9	427	407
				DTA 10 °C/min	Small quantity of Au_2InGa_2	45.4	16.8	37.8	449	
					which disappeared after DTA cycles.					
13	33.1	32.9	34	280 °C, 5 days	Two phase sample					
					$AuIn_2$	35.7	54.9	9.4	432	424
				DTA 10 °C/min	$AuGa_2$	37.8	4.1	58.1		
14	38.3	32.4	29.2	280 °C, 5 days	Primary crystals of				380	367
					$Au_2In\ Ga_2$	42.2	23.5	34.3	395	369
				DTA 10 °C/min	Nucleation of $AuIn_2$	35.3	55.7	9.0	434	427
					Very small quantity of AuIn	52.0	45.3	2.7		
15	46.7	47.7	5.6	280 °C, 5 days	Primary crystals of AuIn	52.9	43.9	3.5	379	445
					Nucleation of $AuIn_2$	36.8	62.8	0.4	467	452
				DTA 10 °C/min	Very small quantity of				484	
					Au_2InGa_2 (pre-DTA)	44.5	19.9	35.6		
16	42.4	29	28.6	280 °C, 5 days	Primary crystals of					
					Au_2InGa_2 and	44.8	22.9	32.3	375	355
				DTA 10 °C/min	$AuIn_2$	36.5	54.5	9..0	387	369
					Nucleation of AuGa and	55.4	2.4	42.2	390	394
					AuIn	53.4	43.2	3.4		
17	41	30.1	28.8	280 °C, 5 days	Primary crystals of					
					Au_2InGa_2 and	44.4	21.9	33.7	372	355
				DTA 10 °C/min	$AuIn_2$	36	55.2	8.8	385	372

					Nucleation of AuGa and AuIn	52.9 52.5	3.2 44.3	43.9 3.2	391	383
18	68.3	4	27.7	280 °C, 26 days DTA 10 °C/min	Primary crystals of Au_7Ga_3 AuGa	 73.8 56.2	 4.6	 21.6 43.8	 299 325	 282
19	73	4.8	22.2	280 °C, 26 days DTA 10 °C/min	Primary crystals of Au_7Ga_3 Au_7Ga_2 (not observed in EDS but verified by XRD)	73.5	4.2	22.3	337	329 335
20	84.7	3.2	12	280 °C, 26 days DTA 10 °C/min	Primary crystals of fcc Au_7Ga_2	 88.7 80.7	 4.9	 6.3 19.3	390 458 740	392 438 754
21	79.7	10	10.3	280 °C, 26 days DTA 10 °C/min	Primary crystals of D024 Au_7Ga_2	 84 78.3	 12.1 3.6	 3.9 18.1	350 530 575 627	347 513 547 631
22	72.9	24.9	2.2	280 °C, 26 days DTA 10 °C/min	Primary crystals of Au_3In Some quantity of Au_7In_3	76.5 71.6	23.5 26.2	 2.2	430 473 516	426 471 512
23	68	23	9	280 °C, 26 days DTA 10 °C/min	Primary crystals of Au_7In_3 Nucleation of AuGa	70.5 55.4	23.1 0.6	6.4 44.0	305 419	392
24	63	28	9	280 °C, 26 days DTA 10 °C/min	Primary crystals of Au_3In_2 Some quantities of Au_7In_3 and AuGa	64.0 70.1 55	31.8 25.9 1.8	4.2 4.0 43.2	305 398	307 389
25	43.9	21.9	34.2	280 °C, 26 days DTA 10 °C/min	Primary crystals of Au_2InGa_2 AuIn AuGa	 41.8 51 53.4	 21.2 45.8 2.7	 37 3.2 43.9	 375 393	 363 371 379
26	73.8	16.9	9.2	280 °C, 26 days DTA 10 °C/min	Crystals of Au_3In Unindexed (maybe Au_7Ga_2 according to modeling)	78.8 75	21.2 13.4	 11.6	344 382 442 490	348 497

Table 2. A list of invariant reactions which are identified by the DTA thermograms. The type P reaction means both ternary peritectic and quasi-peritectic reactions, E means ternary eutectic reactions while e means quasi-binary eutectic reactions. The numbering of the reactions is consistent with the thermodynamic modeling which is considered in a separate report.

Reaction	**T/ °C**	**Type**
$L + AuIn_2 + AuGa_2 \leftrightarrow Au_2InGa_2$	394	P9
$L + AuIn_2 + Au_2InGa_2 \leftrightarrow AuIn$	386	P11
$L \leftrightarrow AuIn + Au_2InGa_2 + AuGa$	373.5	E3
$L \leftrightarrow AuIn_2 + AuGa_2$	432	e2
$L \leftrightarrow AuIn + AuGa$	383	e1
$L + AuIn \leftrightarrow Au_3In_2 + AuGa$	327	P8
$L \leftrightarrow Au_3In_2 + Au_7In_3 + AuGa$	305	E1

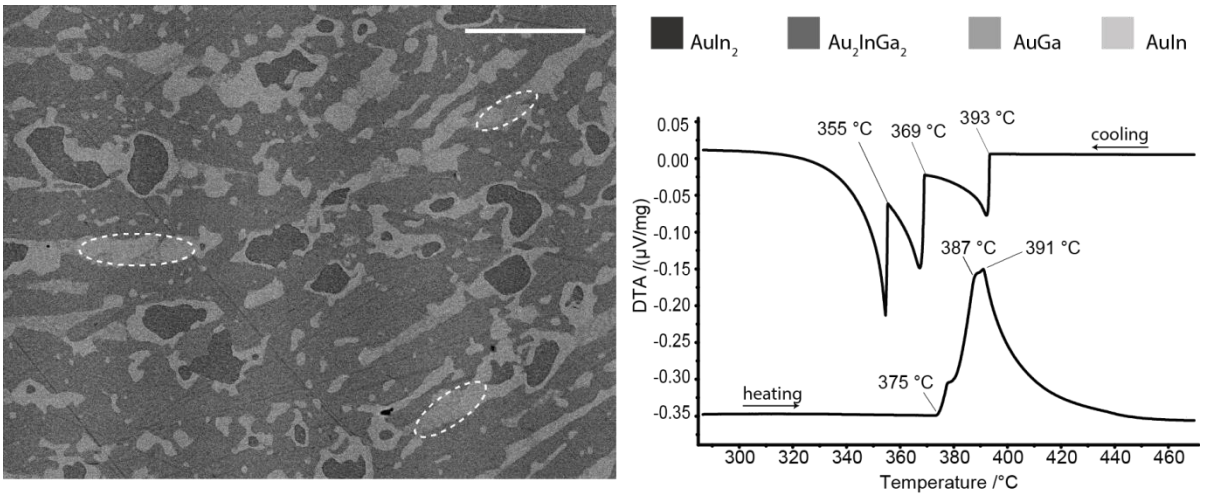

Figure 2. The SEM image and the DTA thermogram (at the rate of 10 °C/min) of sample 16 (42.4 at.% Au, 29.0 at.% In, 28.6 at.% Ga). The four phases $AuIn_2$ (the darkest), Au_2InGa_2, AuGa and AuIn (the lightest) are indicated with different shades of gray. However, AuGa is not easy to distinguish because, as indicated by dashed white lines, it is surrounded by AuIn phase. The scale bar shows 20µm.

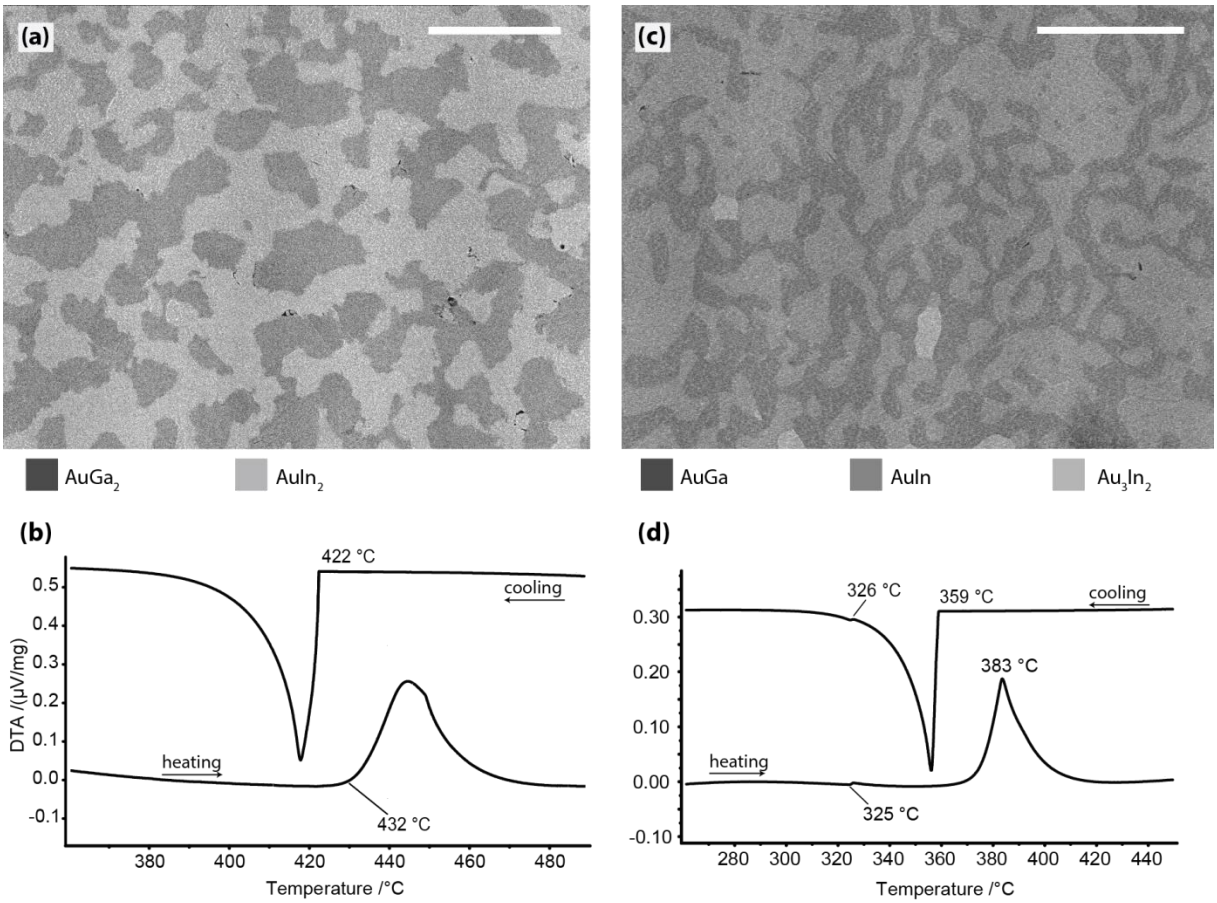

Figure 3. (a) The SEM image and (b) DTA thermogram of sample 13 (33.1 at.% Au, 32.9 at.% In, 34.0 at.% Ga) shows the eutectic reaction in the $AuIn_2$-$AuGa_2$ two phase field. (c) The SEM image and (d) the DTA thermogram of sample 8 (49.9 at.% Au, 25.0 at.% In, 25.1 at.% Ga) shows the eutectic reaction between AuIn and AuGa phases. Both heating and cooling DTA have been recorded with the rate of 10°C/min. Scale bars show 20 µm.

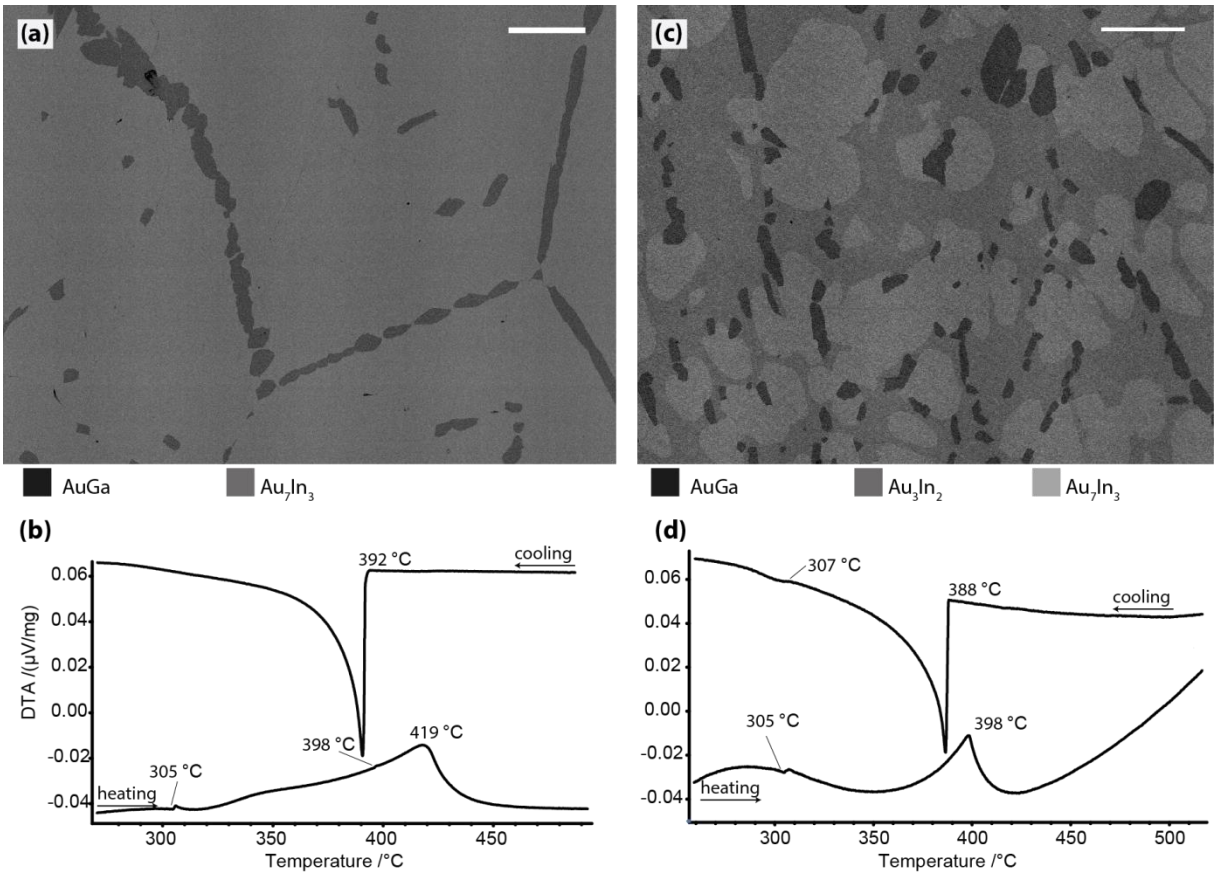

Figure 4. (a) The SEM image and (b) the DTA thermogram of sample 23 (68 at.% Au, 23 at.% In, 9.0 at.% Ga) shows the AuGa-Au_7In_3 two phase field. (c) The SEM image and (d) the DTA thermogram of sample 24 (63 at.% Au, 28 at.% In, 9.0 at.% Ga) shows the AuGa-Au_3In_2-Au_7In_3 three phase field. Both heating and cooling DTA have been recorded with the rate of 10°C/min. Scale bars show 50 μm.

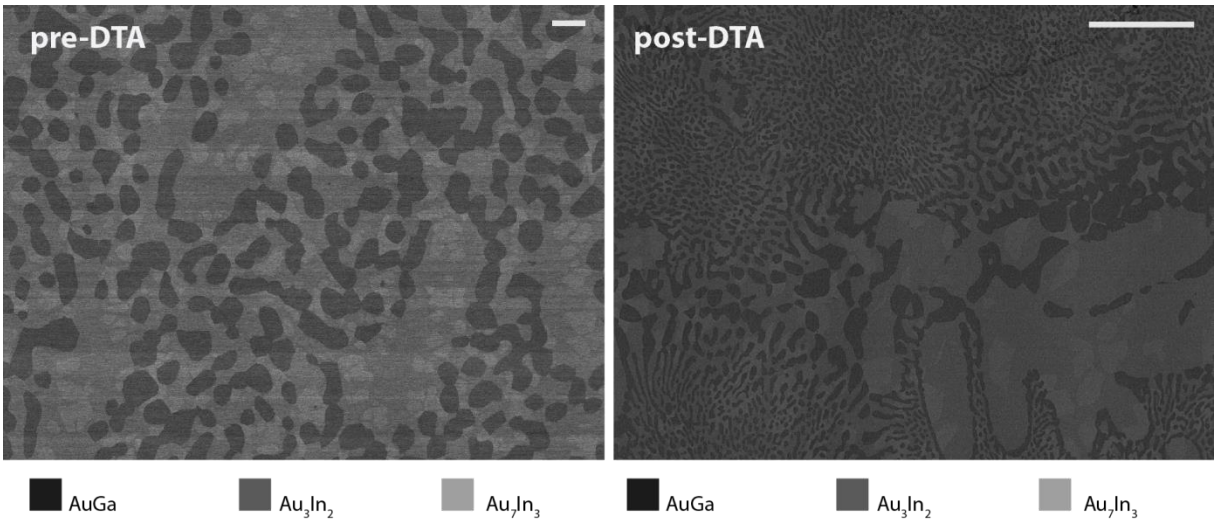

Figure 5. Micrographs of sample 3 (57.3at.%Au, 22.8at.%In, 19.9at.%Ga) before and after DTA measurements show the same coexisting phases with different grain size and microstructural patterns. The scale bar shows 20 µm.

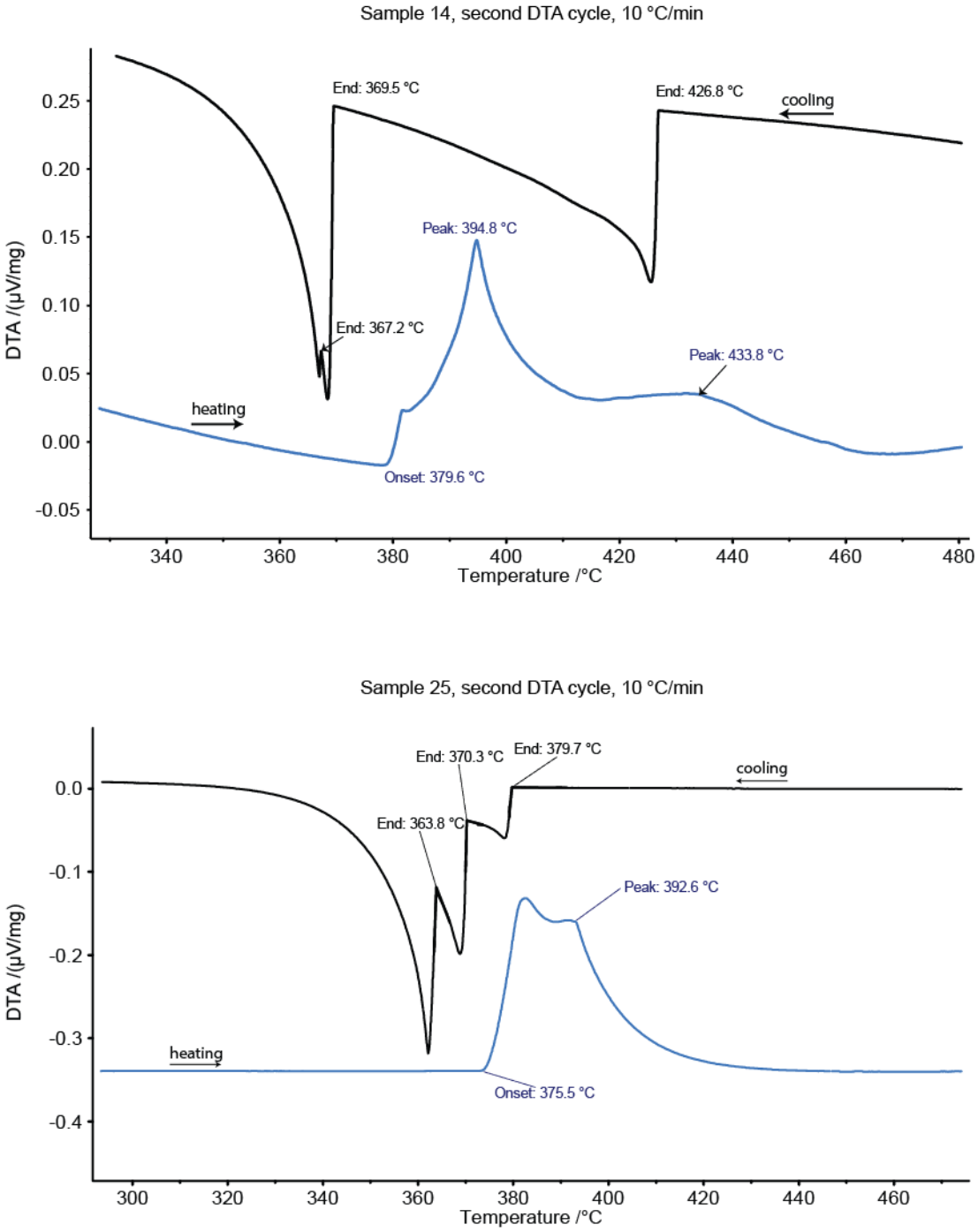

Figure S1. Both DTA thermograms of sample 14 (38.3 at.%Au, 32.4 at.%In, 29.2 at.%Ga) and 25 (43.9 at.%Au, 21.9 at.%In, 34.2 at.%Ga) show the occurrence of a thermal event at slightly above 390 °C which is related to the formation of the Au_2InGa_2.

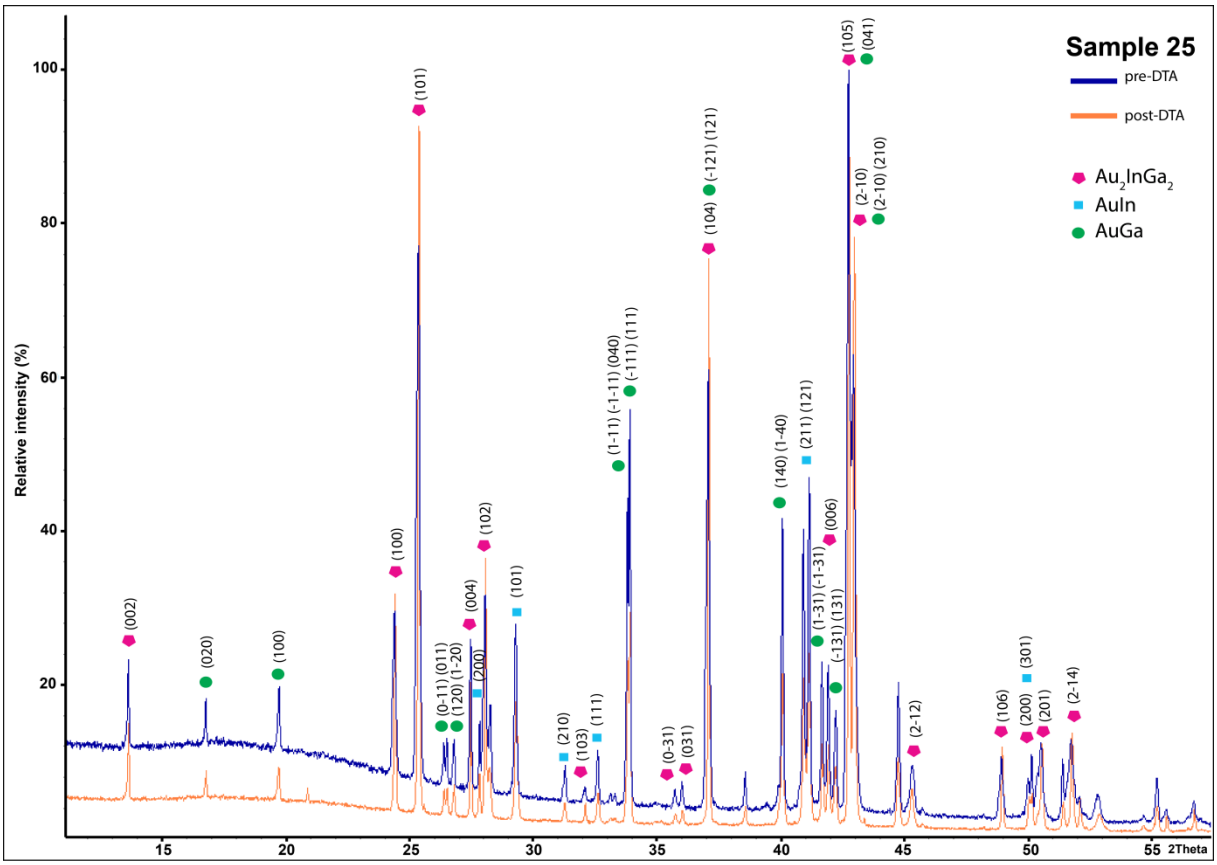

Figure S2. Pre- and post-DTA powder pattern of sample 25 with the composition of 43.9 at.%Au, 21.9 at.%In, 34.2 at.%Ga.